A Study upon Tsunami and Typhoon Surge via Spectrogram of Tide Wave

Yih Nen Jeng (鄭育能)
Department of Aeronautics and Astronautics, National Cheng Kung University
Yueh-Jiuan G. Hsu (徐月娟)
Marine Meteorology Center, Central Weather Bureau

Abstract

Two tide wave data of Cheng-kong harbor at Taitung, Taiwan are examined by a Fourier sine spectrum and a new time frequency transform. The first data string, which covers the period from August 1st, 2002 to July 31th, 2004, employed a sampling time interval of 6 minutes. The second string ranges from December 9th to 11th and has a sampling rate of 6 data per minute. The main concerning involves the tsunami and typhoon surge waves within the data. The transform involves three steps: use the iterative Gaussian smoothing method to extract data within the interested frequency range; evaluates the Fourier sine spectrum; and then imposes a window to the spectrum at a given frequency whose inverse Fourier transform is corresponding to the real part of the spectrogram. The tsunami tide information has been obtained by comparing the 10 seconds and 6 minutes sampling interval. It seems that the tsunami wave measured in the harbor involves the water level decreasing, increasing and oscillation stages. The time frequency transform shows that the oscillatory period, which has three dominant modes, ran over a period about 10 hours. These details can only be checked after removing the smooth part. As to the typhoon surge, not much information can be extracted by the present analysis.

Key word: Tsunami tide, typhoon surge, time frequency analysis

1. Introduction

Because of the development of computer hardware and software, the capability of collecting long data strings is rapidly increasing. Engineering applications of these data heavily rely on the understanding of the involved details. It seems that the most convenient tools to look into details embedded in a data string are the Fourier spectrum and short time Fourier transformation. The form method can be evaluated via the Fast Fourier Transform (FFT) and reflects the overall sinusoidal information. The latter one shows the time-dependent distributions of both amplitude and frequency [1-7].

It is well known that both the Fourier and short time Fourier transforms had already been proven to be complete expansions. In spite of the fact that a data string collected from nature, such as earthquake, underground water level, and tide data, frequently involves complicated details emitted from multiple sources, these two transforms can faithfully capture all the desired insights whenever they are properly employed. In this study, the tide data involving the tsunami and typhoon will be examined by these two transforms.

If the FFT is employed to find the spectrum of a continuous data string, the result frequently involves the Direct Current (DC) contamination and error due to the non-periodic condition. Moreover, if one tries to remove the non-sinusoidal part embedded in the data string via a non-diffusive filter, the resulting sinusoidal data may be contaminated by the phase shift introduced by the filter. This study will employ the diffusive filter of Ref.[8-10] to decouple the non-sinusoidal part and/or extract the high frequency part of the tsunami data. Then, the Fourier sine spectrum generator of Ref.[6,7] is employed to find the spectrum free from the error induced by the non-periodic condition. In Ref.[11-14], it had been shown that the Gabor transform can be approximated by a new approach without directly evaluating the convolution integral and is free from the corresponding numerical integration error. This study will employ this new approach to evaluate the spectrogram.

2. Theoretical Developments

For the sake of completeness, all the required tools are briefly reviewed below.

2.1 Iterative Gaussian Smoothing Method

Assume that a discrete data string can be approximated by [13,14]

$$y_j = \sum_{l=0}^{\infty}[b_l \cos\frac{2\pi t_j}{\lambda_l} + c_l \sin\frac{2\pi t_j}{\lambda_l}] + \sum_{n=0}^{N} a_n t_j^n, \qquad (1),$$

where the polynomial represents the non- sinusoidal part, $-\infty < j < \infty$, and N is referred to as the largest power for which $a_n \to 0$ for all $n > N$. Note that the non-sinusoidal part may be interpreted as the sum of monotonic part and all the Fourier modes whose

wavelength longer than the expansion interval. When the Gaussian smoothing method is employed, the following formulas are obtained [8-10].

$$\bar{y}_j \approx \frac{1}{\sqrt{2\pi}\sigma}\sum_{i=-\infty}^{\infty}\exp[-\frac{(i-j)^2(\Delta t)^2}{2\sigma^2}]y_i \qquad (2),$$
$$y'_j = y_j - \bar{y}_j \quad -\infty < j < \infty$$

where $\bar{y}_j$ and y'_j are the smooth and high frequency parts, respectively. In Ref. [13,14], it was proven that after applying the Gaussian smoothing method once, the resulting smoothed data becomes

$$\bar{y}(x) = a_N x^N + a_{N-1}x^{N-1} + \sum_{n=0}^{N-2} e_n x^n + \sum_{l=0}^{\infty} a(\sigma/\lambda_l)\{b_l\cos\left(\frac{2\pi t}{\lambda_l}\right) + c_l \sin\left(\frac{2\pi t}{\lambda_l}\right)\} \qquad (3),$$

where the upper index $[N/2]$ is the Euler number which takes the integer part only and the attenuation factor satisfies [8-11]

$$0 \le a(\sigma/\lambda_l) \approx \exp[-2\pi^2\sigma^2/\lambda_l^2] \le 1+\varepsilon \qquad (4),$$

where ε is the machine error of the computing device. Then the high frequency part becomes

$$y'(t) \approx \sum_{n=0}^{N-2}[e_n - a_n]x^n + ... = \sum_{n=0}^{N-2} g_n x^n + \sum_{l=0}^{\infty} a(\sigma/\lambda_l)\{b_l\cos\left(\frac{2\pi t}{\lambda_l}\right) + c_l \sin\left(\frac{2\pi t}{\lambda_l}\right)\} \qquad (5),$$

Obviously the degree of the polynomial is reduced by 2. If the high frequency part is repeatedly smoothed m times by the Gaussian smoothing method, where $m > N/2$, the corresponding results can be rearranged in the followings [8-11].

$$y'_m = \sum_{l=0}^{\infty}[1-a(\sigma/\lambda_l)]^m\left[b_l\cos\left(\frac{2\pi t}{\lambda_l}\right) + c_l\sin\left(\frac{2\pi t}{\lambda_l}\right)\right]$$
$$\bar{y}(m) = \bar{y}_1 + \bar{y}_2 + ... + \bar{y}_m = y - y'_m = \sum_{l=0}^{N} A_{l,m,\sigma}[b_l\cos(2\pi t/\lambda_l) + c_l\sin(2\pi t/\lambda_l)] \qquad (6),$$

where y'_i and $\bar{y}_i$ are the high frequency and smoothed parts at $i-$th smoothing step, respectively. Finally, $\bar{y}(m)$ is the desired smooth part and y'_m is the desired high frequency part which completely removes the non-sinusoidal part. Obviously, both the original Gaussian smoothing and iterative smoothing algorithms are approximately diffusive.

For a real data string, the infinite upper bond of Eqs.(2-6) becomes M which reflects the data size. The finite data size will induce smoothing error around the two ends. In Ref.[14], the following empirical relation is proposed to estimate the faded range of $1 \le m \le 10^4$.

$$x_{0.001}/\sigma \approx 3.4 + 2.83\log_{10}(m) \qquad (7),$$

where $x_{0.001}$ is the distance from an end point where the resulting y'_m has at least a 0.1% deviation from that estimated by Eq.(6). In other words, the error penetration distance increases exponentially with respect to the number of iteration cycle.

Suppose that all the waveforms within the range of $\lambda_1 < \lambda < \lambda_2$ are insignificantly small. It is intuitive to require that

$$[1-a(\sigma,\lambda_1)]^m \approx \left[1-\exp\left\{-2\pi^2\sigma^2/\lambda_1^2\right\}\right]^m = 1-\delta$$
$$[1-a(\sigma,\lambda_2)]^m \approx \left[1-\exp\left\{-2\pi^2\sigma^2/\lambda_2^2\right\}\right]^m = \delta \qquad (8),$$

where the parameter δ can take an arbitrarily small value. The solution of this set of simultaneous equations will give the value of the smoothing factor σ and the number of cycles, m, required to perform the decomposition of the two waves. In this study, $\lambda_2/\lambda_1 = 2$ and $\delta = 0.001$ are employed so that the parameters are $\sigma/\lambda_1 = 0.7715$ and $m \approx 127$.

In Ref.[14], in stead of directly employing Eq.(2) and the iteration procedure on the time domain. The following fast version on the spectral domain had been developed.

1. Properly choose two end points of the data string and connect them with a straight line.
2. Substrate the straight line from the original data string.
3. Find the Fourier spectrum via an FFT algorithm.
4. Determine the transition zone λ_2/λ_1 where $\lambda_1 < 0.05T$. Solve Eq.(7) to obtain σ and m for a given δ.
5. Multiple every Fourier mode by the factor
$$b(\sigma,\lambda_l,m) = \left[1-\exp\left\{-2\pi^2\sigma^2/\lambda_l^2\right\}\right]^m \qquad (9)$$
6. Evaluate the inverse FFT of the resulting spectrum to obtain the desired high frequency part.
7. The difference between the original data and high frequency part is the smooth part.

This procedure employs the linear trend removal [5] as an enhance technique to reduce the error around the two ends. Consequently, the resulting error region is slightly smaller than that estimated by Eq.(7). Moreover, this procedure can be strictly diffusive because every Fourier mode of the high frequency part is embedded by the attenuation factor satisfying the relation

$$0 \le b(\sigma,\lambda_l,m) \le 1 \qquad (10)$$

In order to avoid the possibility of ruining these criteria by the round-off error, $b(\sigma,\lambda_l,m)$ can be artificially restricted via programming technique so as to satisfy Eq.(10).

Since the fast version skips the application of Eq.(2) and iteration procedure, the required computing resource includes: the forward and backward FFTs for the evaluation of Fourier spectrum ($2M\ln_2 M$) and the evaluation of modifying amplitude of every Fourier mode ($<100M$). It means that the required computing resource is slightly longer than two times of employing the FFT.

2.2 Fourier Sine Spectrum Generator

In general, if an FFT algorithm is employed to evaluate the spectrum of a data string with non-sinusoidal part, the resulting spectrum always has an exponentially decayed envelope. The information of the low frequency part is thus seriously contaminated. Similarly, the non-periodic condition often introduces a negative contribution. In Ref. [8-11], the above iterative filter is first employed to remove the non-sinusoidal part and then reduce the non-periodic condition's error via the following procedure.

1. Use the fast filter to remove all the short modes whose wavelengths are less than 2 to 3 times of the sampling interval. Now the linear trend removal is not necessary. The resulting response will be a smooth data string.
2. Employ the above mentioned fast and sharp filter to remove the non-sinusoidal part.
3. For the remaining high frequency part, use search and interpolation methods to find 0 points around the two ends.
4. Use the monotonic cubic interpolation [7-11,15] to redistribute the data and let the total number of points is set to be 2^K, where K is an integer ($2^K > 2M$) to make sure that the interpolation error is small enough.
5. Perform an odd function mapping with respect to a new end so that the final data point is doubled.
6. A simple FFT algorithm is employed to generate the Fourier sine spectrum.

2.3 Fourier Sine Spectrogrum Generator

It can be proven that the Gabor transform of $y(t)$ using the Gaussian kernel, the following formulas can be easily proven [13,14].

$$G(f,\tau) = 1/\sqrt{a}\int_{-\infty}^{\infty} y(t)e^{-2i\pi f(t-\tau)}e^{-(t-\tau)^2/(2a^2)}dt \approx \sqrt{\pi a/2}\sum_{l=0}^{L-1} e^{-2\pi^2 a^2(f_l-f)^2}(b_l - jc_l)e^{2i\pi f_l \tau} \quad (11),$$

The direction of the first identity will lead to a first order accurate numerical integration because the data $y(t)$ is always discrete. Because of the orthogonal property of both the FFT and inverse FFT of a periodic $y(t)$, the second relation of Eq.(11) will involve the round-off error only. Therefore, this study employs the second formulation to attain a version of mall integration error.

3. Results and Discussions

In the tide data string of the Cheng-kong harbor (from August 1st, 2002 to July 31th, 2004), there was a tsunami record in December 10th, 2003. Around the day of 2003/09/01, there was a typhoon surge. The whole data string is shown in Fig.1a and two detailed plots of the original data around the surge and tsunami are shown in Figs.1b and 1c, respectively. In Fig.1d, the 3 days data around the tsunami with a sampling rate is shown (from 2003/12/09 to 2003/12/11).

From Figs.1a and 1b, one can find the instance of the typhoon surge but can not identify the tsunami from Fig.1c because the latter is a minor impulsive data as show in Fig.1d. In order to inspect the tsunami data, the iterative Gaussian smoothing method with $\sigma = 0.05$ days and $m = 126$ is employed to remove all the long wave part of the original data of Fig.1b. The resulting high frequency part of the data with 6 minutes sampling rate is shown as the heavy solid line in Fig.2a where the corresponding data of 10 seconds sampling rate is shown as the thin solid line. Those shown in Fig.2b are the 6 minute data, 10 second data and its smoothed part with parameters of $\sigma = 0.003$ days and $m = 126$. Both data show that there are three steps of the tsunami wave: the water level is first slightly decreased, next is the incremental period and then followed by water level oscillation. The long second and the oscillatory third steps might be induced by the harbor effect of reserving excessive water within a short period. The 6 minutes data string has a long water level decreasing period (about 45 minutes) may be caused by the insufficient sampling rate. On the other hand, the smoothed part of the 10 seconds data string has a water level decreasing period of about 15 minutes. Note that this period is also approximately the period between two successive peaks of the oscillatory period.

The Fourier sine spectra of the period of 39.4-40.2 seconds of the high frequency part of both data strings are shown in Figs.2c and 2d, respectively. These spectra reflect the oscillatory behavior within the harbor induced by the tsunami tide. It seems that both spectra have the first dominant modes with the wavelength of about 18 minutes while the second dominant modes have wavelengths of about 11.5 minutes. The second dominant mode of the 6 minute data splits into two nearby modes may be caused by the insufficient sampling rate. It seems that the 15 minutes period is a combination of these two dominant waves. Moreover, the 18 minutes period is closely related to the water level decreasing period identified by other technique.

Two- and three-dimensional spectrograms with window factor of $c = 1$ days (wideband spectrogram) are shown in Figs.3 and 4, respectively. Those shown in Figs.5 and 6 are those with $c = 0.009$ days (narrowband spectrogram). From the former figures, one can grasp the information that, around the incident instance of tsunami wave, there is a vertical contamination band in the spectral direction. The contaminated band is induced by the sudden enlargement of the oscillatory period. From the latter figures with narrowband spectrogram, one can pick up the information of important modes as shown. From these figures, one can clearly see three modes whose wavelengths are 9.23, 11.5, and 18 minutes. The first and second dominant modes (18 and 11.5 minutes modes) are significant in the period from 39.5 to 39.95th days, say about 11 hours. The third mode (9.23 minutes and also 6.5 cycles per hour) exists in the interval from 39.5 to 39.86 days, say about 9 hours. After the time of 40th day, in addition to these modes, there are many other

modes which may be induced by the dissipation of the harbor.

The spectrum of the typhoon surge wave of Fig.1c is shown as the heavy line in Fig.7, where the expansion period covers the range from 390 to 410 days. That shown as thin solid line in the same figure is the spectrum of 355-375 days. From this figure, it seems that the contribution of the typhoon surge wave can not be reflected from spectrum. Those shown in Figs.8 and 9 are two- and three-dimensional spectrograms of the surge wave where the whole day, half, one third, one fourth, and one fifth tides are captured. The surge wave induces a vertical contamination band as shown. Up to this point, not other details can be extracted from these spectrograms because the surge introduces an additional smooth and positive data within one day period approximately. Such a short period addition can be captured by the present time-frequency analysis.

4. Conclusions

The Fourier sine spectrum and spectrogram were successively employed to study a tsunami and a typhoon surge wave of the tide data of the Cheng-Kung harbor in Taidong, Taiwan. From the filtered time-domain data and time-frequency transform, detailed information of the tsunami tide is captured. However, no much information of the surge wave can be obtained from the present tools.

5. Acknowledgement

This work is supported by the National Science Council of Taiwan, R. O. C. under the grant number NSC-96 -2221-E006-186-MY3.

1. M. Farge, "Wavelet Transforms and Their Applications to Turbulence," *Annu. Rev. Fluid Mech.*, vol.24, pp.395-457, 1992.
2. R. Carmona, W. L. Hwang, and B. Torresani, *Practical Time-Frequency Analysis, Gabor and Wavelet Transforms with in Implementation in S*, Academic Press, N. Y. , 1998.
3. *Time-Frequnecy Signal Analysis, Methods and Applications*, ed. by B. Boashash, Longman Cheshire, Australia, 1992.
4. J. S. Bendat, and A. G. Piersol, *Random Data Analysis and Measurement Procedures* 3rd ed., John Wiley & Sons, New York, 2000, Chapters 10 & 11, pp.349-456.
5. W. H. Press, S. A. Teukolsky, W. T. Vetterling, and B. P. Flannery, *Numerical Recipes in C, the Art of Scientific Computing*, 2nd ed., Cambridge Univ. press, 1992.
6. Y. N. Jeng and Y. C. Cheng,"A Simple Strategy to Evaluate the Frequency Spectrum of a Time Series Data with Non-Uniform Intervals," *Trans. Aero. Astro. So., R. O. C.*, vol.36, no.3, pp.207-214, 2004.
7. Y. N. Jeng and Y. C. Cheng, "A New Short Time Fourier Transform for a Time Series Data String," J. of Aero. Astro. And Aviation, Series A, 2007, vol.39, no.2, pp117-128.
8. Y. N. Jeng, P. G. Huang, and Y. C. Cheng, "Decomposition of One-Dimensional Waveform Using Iterative Gaussian Diffusive Filtering Methods, *Proc. Royal Soc. Lon. Series A*, vol. 464, pp.1673-1695, 2008, doi:10.1098/rspa.2007.0031
9. Y. N. Jeng, P. G. Huang, and H. Chen, "Filtering and Decomposition of Waveform in Physical Space Using Iterative Moving Least Squares Methods," *AIAA paper* no.2005-1303, Reno Jan. 2005.
10. Y. N. Jeng and P. G. Huang, "Decomposition of One-Dimensional Waveform with Finite Data length Using Iterative Gaussian Smoothing Method," *Proc. 31th National Conference on Theoretical and Applied Mechanics*, DYU, Changhwa, Taiwan, paper no. ctam 30-389, Dec. 15-16, 2006.
11. Y. N. Jeng, "Time-Frequency Plot of a Low Speed Turbulent Flow via a New Time Frequency Transformation," Proc. 16th Combustion Conf., paper no.9001, April, 2006, Taiwan.
12. Y. N. Jeng and Y. C. Cheng, "A Time-Series Data Analyzing System Using a New Time-Frequency Transform", Proc. 2006 International Conference on Innovative Computing, Information and Control, paper no. 0190, Beijing, China, Sept. 30, 2006.
13. Jeng, Y. N., T. M. Yang, Y. C. Cheng and J. M. Huang, "Acoustic Data Analysis of Remote Control Vehicles via Fourier Sine Spectrum and Spectrogram," paper no. AIAA2008-4263, Jun 23-26, 2008.
14. Jeng,Y. N., "Diffusive and Fast Filter Using Iterative Gaussian Smoothing," *Proc. 18th Combut. Conf.*, paper X001, March, 2008, Taiwan.
15. H. T. Huynh, "Accurate Monotone Cubic Interpolation," SIAM J. Number. Anal. vol.30, no.1, pp57-100, Feb.1993.

(a)

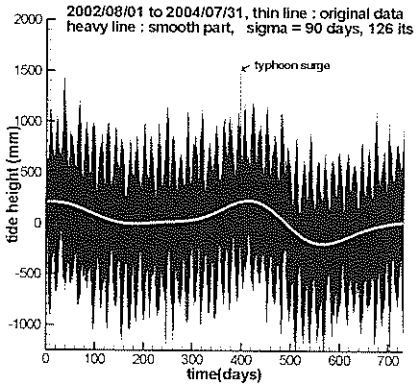

(b)

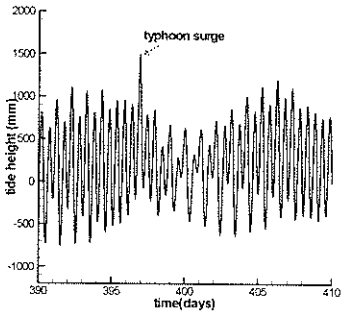

(c)

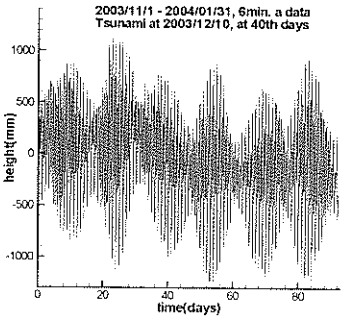

(d)

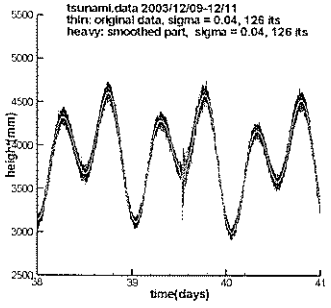

Fig.1 original data: (a) the whole data string of the first data (6 minutes sampling rate); (b) data around the typhoon surge; (c) data around the tsunami; and (d) data around the tsunami (10 seconds sampling rate)

(a)

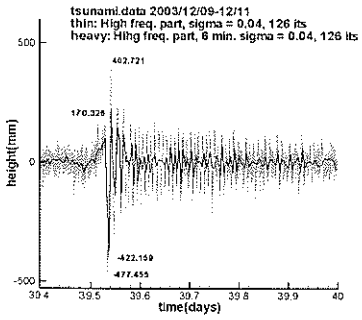

(b)

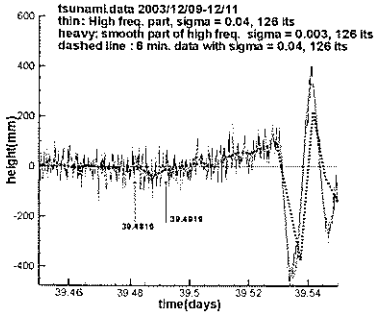

(c)

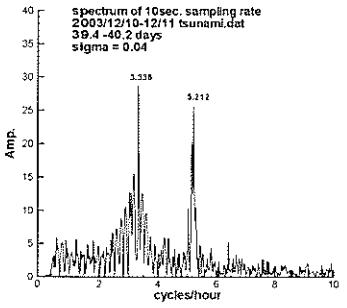

(d)

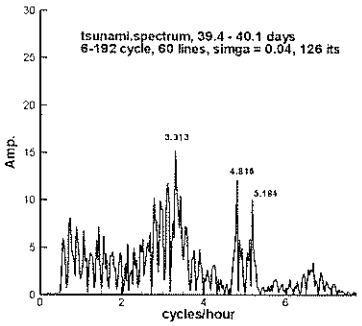

Fig.2 The tsunami data: (a) comparison of high frequency part of two data with different sampling rate; (b) detailed plots; (c) spectrum of 10 seconds sampling rate; and (d) spectrum of 6 minutes sampling rate.

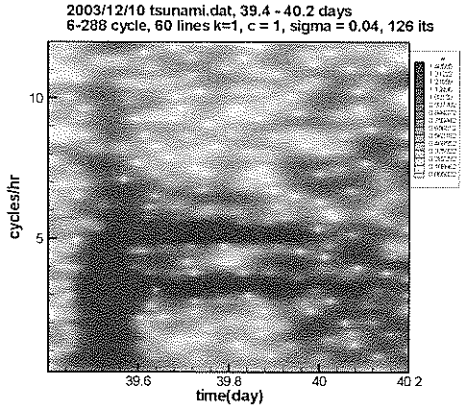

Fig.3 The two-dimensional amplitude plot of the spectrogram of the tsunami tide, 39.4 – 40.2th days, window factor $c = 1$

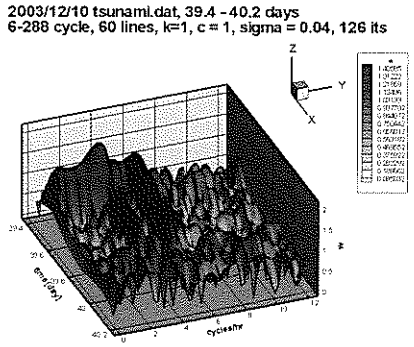

Fig.4 The three-dimensional amplitude plot of the spectrogram of the tsunami tide, 39.4 – 40.2th days, window factor $c = 1$

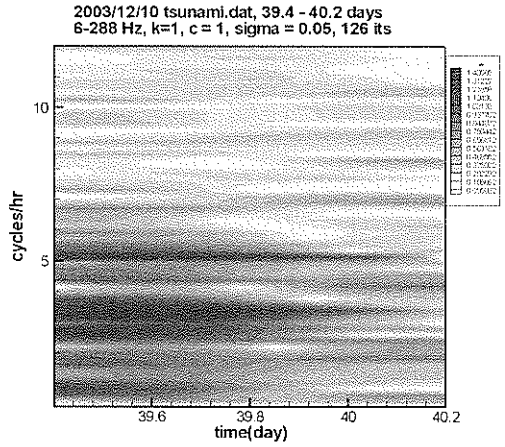

Fig.5 The two-dimensional amplitude plot of the spectrogram of the tsunami tide, 39.4 – 40.2th days, window factor $c = 0.009$

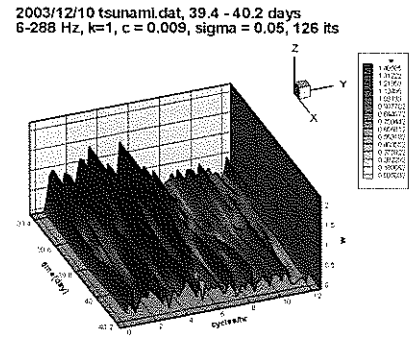

Fig.6 The three-dimensional amplitude plot of the spectrogram of the tsunami tide, 39.4 – 40.2th days, window factor $c = 0.009$

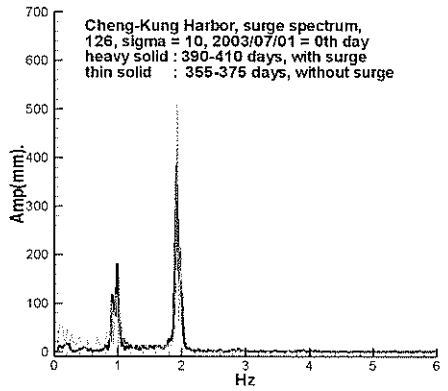

Fig.7 Spectra comparison: spectrum of Fig.7 (heavy solid) and spectrum without surge (thin solid).

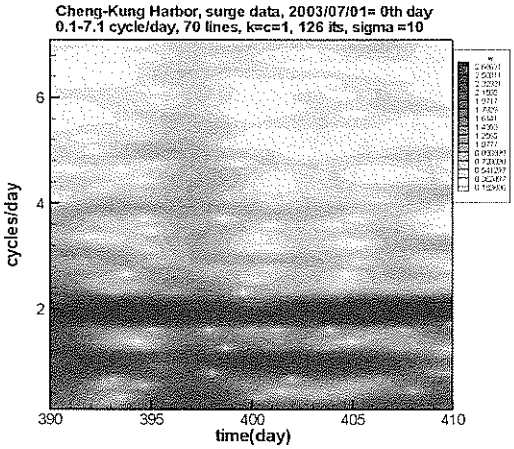

Fig.8 The two-dimensional amplitude of the spectrogram of the typhoon surge.

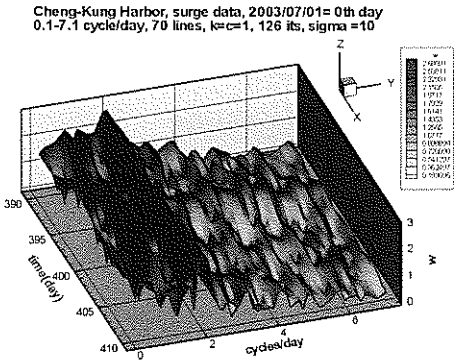

Fig.9 The three-dimensional amplitude of the typhoon surge's spectrogram.